

# Effects of meteorology on long-range nonlinear propagation of jet noise from a static, high-performance military aircraft

Kent L. Gee, Brent O. Reichman and Alan T. Wall

Citation: [Proc. Mtgs. Acoust.](#) **35**, 040006 (2018); doi: 10.1121/2.0001531

View online: <https://doi.org/10.1121/2.0001531>

View Table of Contents: <https://asa.scitation.org/toc/pma/35/1>

Published by the [Acoustical Society of America](#)

---

---



**Advance your science and career  
as a member of the**

**ACOUSTICAL SOCIETY OF AMERICA**

LEARN MORE



---

## **Effects of meteorology on long-range nonlinear propagation of jet noise from a static, high-performance military aircraft**

**Kent L. Gee and Brent O. Reichman**

*Department of Physics and Astronomy, Brigham Young University, Provo, UT, 84602; [kentgee@byu.edu](mailto:kentgee@byu.edu);  
[brent.reichman@gmail.com](mailto:brent.reichman@gmail.com)*

**Alan T. Wall**

*Air Force Research Laboratory, Wright-Patterson Air Force Base, OH, 45433; [alan.wall.4@us.af.mil](mailto:alan.wall.4@us.af.mil)*

Nonlinear propagation of noise from military jet aircraft has been fairly well documented, but only within a few hundred meters from the aircraft. This paper describes analysis of nonlinear propagation for morning static runups of F-35 aircraft at greater distances, out to 1220 m near the direction of maximum radiation and at heights ranging from 0 m up to 30.5 m. A comparison of overall levels with distance and height reveals evidence of significant atmospheric refraction effects, and a general trend of decreasing level with height. Examination of nonlinearity metrics reveals opposite behavior, however. At these distances, nonlinear propagation effects are often strongest in waveforms with lower sound levels, which is counterintuitive. One important finding, however, is that acoustic shock strength can vary greatly from runup to runup, even for seemingly small changes in atmospheric conditions. This analysis demonstrates the need for further research into long-range nonlinear propagation of jet noise through realistic atmospheric conditions.

---

## 1. INTRODUCTION

To predict long-range noise exposure from military aircraft, an accurate representation of far-field levels is required. To this end, prior measurements<sup>1</sup> of an F-35 sound field included microphone locations up to 1220 m (4000 ft) away from the aircraft. However, long-range acoustic propagation introduces factors that can increase uncertainty and complicate predictions.<sup>2,3</sup> While an ANSI jet noise measurement standard<sup>4</sup> specifies a range of allowable weather conditions to help reduce some of this uncertainty, sufficient latitude still exists such that overall level, spectral shape, and waveform characteristics may vary considerably over ground-to-ground during allowable conditions. This paper demonstrates large weather-related variations in overall sound pressure level (OASPL) and nonlinearity metrics at distances beyond 305 m. Quantifying these changes is important for predicting jet noise perception.

Minor changes in atmospheric conditions can significantly affect both the propagation medium and acoustic propagation paths. Variability in atmospheric pressure, humidity, and temperature affects atmospheric absorption, which over large distances can significantly alter high-frequency content.<sup>5</sup> However, larger spectral changes closer to the peak-frequency region of jet noise can result from multipath effects. These multipath effects can be caused by ground reflections; however, more complex multipath effects at distances greater than around 100 m may be caused by a refractive atmosphere.<sup>6,7</sup> For example, Salomons<sup>8</sup> showed a case of a “typical” downward refracting atmosphere that resulted in 40 possible ray paths between two sources 1000 m apart. Upward, downward, and upward-downward<sup>9</sup> refracting atmospheres can be further complicated by turbulence, which smears out interference nulls and scatters sound to shadow zones.<sup>8,10</sup> In addition, nonlinear propagation must be taken into account for high-power engine conditions, and relatively little research has been conducted to showing the effect of these atmospheric conditions on details of shock formation and propagation.<sup>11</sup>

This paper describes far-field measurements of a stationary F-35 and effects of atmospheric conditions on OASPL, spectra, and nonlinearity metrics. These quantities and their uncertainty are shown at distances from 39 m to 1220 m from measurements that took place over two days. Spectra and nonlinearity metrics point to the importance of nonlinear propagation at large distances from the source, with significant shocks still present at 610 and 1220 m from the source. Far-field data show the presence of multipath interference effects that likely indicate that for the majority of the experiment, a downward-refracting atmosphere was present. OASPL and nonlinearity metrics are considered as a function of height at distances of 610 and 1220 m, with the surprising result that while for the bulk of the experiment OASPL tends to decrease with height, nonlinearity indicators tend to increase. Evidence is shown of a transition from a downward-refracting atmosphere to an upward-refracting atmosphere, resulting in changes of over 10 dB at microphone heights close to the ground. Occasional outliers point to the fact that some circumstances may produce significantly increased shock content.

## 2. MEASUREMENTS

The microphone layout for this experiment has already been described in detail elsewhere.<sup>1</sup> However, as this paper deals more with long-range propagation effects and the effects of weather conditions, certain features of the measurement array are highlighted here. In particular, six measurement locations (with two locations featuring multiple microphones at varying heights) at 610 m (2000 ft) and 1220 m (4000 ft) from the microphone array reference point (MARP, located ~7 m behind the nozzle exit) are shown in Figure 1. These measurement locations are along the 120°, 135°, and 150° radials, allowing for comparisons in the extreme far field. The measurement locations at 120° and 150° at both distances were limited to a single microphone 9.1 m (30 ft) above the ground, while cranes were located at 135°, allowing measurements at heights of 0, 1.5, 6.1, 9.1, 22.9, and 30.5 m (0, 5, 20, 30, 75, and 100 ft) above the ground at both distances. Also shown in Figure 1 are three weather measurement locations at 61, 152, and 250 m (200, 500, and 820 ft) from the MARP. A single weather station was placed 1.5 m (5 ft) above the ground at 61 m from the MARP, while the 152 m location had weather stations at heights of 1.5, 3.1, and 6.1 m and the 250 m location had weather stations at heights of 0.31, 1.5, 3.1, and 6.1 m. However, the ordering of station heights is unknown because of discrepancies in the measurement documentation, so while the data represent a wide range of measurement locations, weather data are simply averaged for the purposes of this paper.

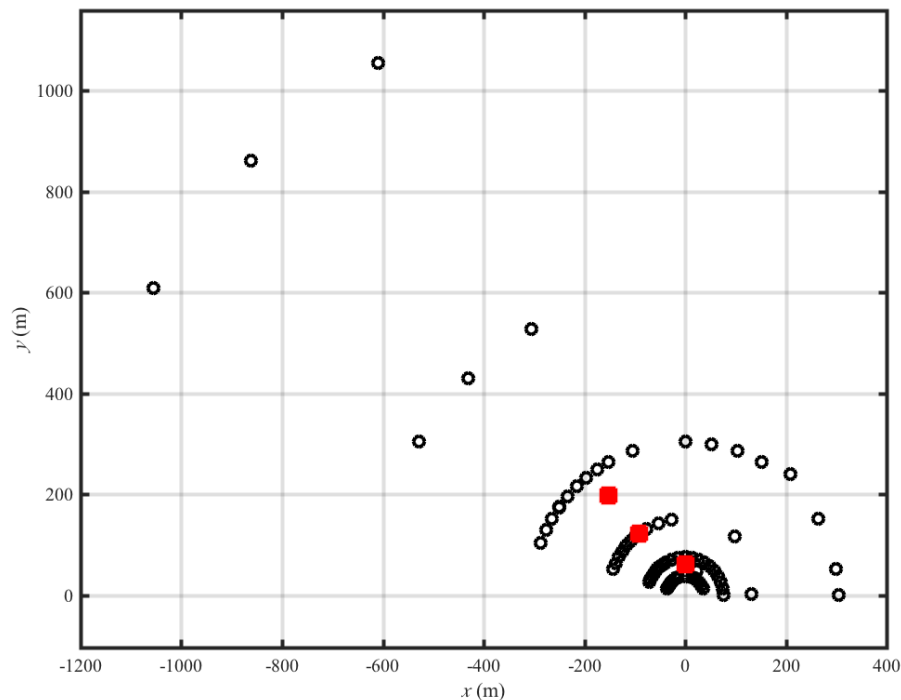


**Figure 1.** Microphone locations for ground run-up measurements at distances of 38 m and greater relative to the MARP, located at  $(x, y) = (0, 0)$ . Also shown as red squares are locations of weather stations, with weather stations present at multiple heights for the two farther locations.

Individual measurements (runs) lasted roughly 30 seconds, with 9-10 runs for each engine condition. Run numbers in the 100s correspond to runs on the first day of measurements (F-35A) while run numbers in the 200s correspond to the second day (F-35B). James *et al.*<sup>1</sup> have shown the acoustical equivalence of the two aircraft. Average weather conditions for all of the runs at 100% engine thrust request (ETR) are shown in Table 1, along with the required range of weather conditions allowed in the standard. This allowed range of weather values is representative of all runs measured. Most parameters were steady throughout the measurement, with temperatures ranging from 20.0-22.7°C and relative humidity staying between 40-44%. Wind varied more than these parameters, but during measurement times stayed under the threshold of a maximum wind speed of 8.0 kts. There were more significant wind events during the first day of measurements, with some events reaching an average of over 6.0 kts. Sunrise on both measurement days occurred just before a local time of 6:30 AM, meaning that some runs took place before dawn and some after, which may be important when considering effects of a possible temperature inversion or lapse.

**Table 1.** Station-averaged weather conditions for all recorded runs at 100% ETR for both measurement days and ranges given in the standard.

Run	114	119	124	129	207	213	219	225	231	243	Standard
Time (A.M.)	6:08	6:42	7:15	7:48	5:10	5:23	5:37	5:50	6:04	7:34	N/A
Temp. (°C)	22.7	22.0	21.7	22.2	20.9	20.9	20.9	20.5	20.0	20.3	2.2 - 35
Wind (kts)	5.7	1.3	3.2	6.5	2.4	2.4	2.0	1.8	1.4	2.0	0 - 8.0
RH (%)	41.1	43.7	42.1	40.3	41.1	42.3	42.7	42.7	44.9	40.2	10 - 95%

### 3. METRICS

Nonlinearity metrics used by Reichman *et al.*<sup>12</sup> to characterize F-35 shocks for distances up to 305 m are again considered here for longer range propagation, along with the OASPL. While a large OASPL is not by itself a direct indicator of shock content, increasing OASPL is associated with enhanced nonlinear propagation for all other things being equal. Its changes due to long-range propagation effects are shown here, along with three

nonlinearity parameters: the derivative skewness, average steepening factor (ASF), and shock energy fraction (SEF). Variations across runs are quantified to show how the different metrics are affected by long-distance variations in atmospheric propagation.

### A. DERIVATIVE SKEWNESS

The skewness of the pressure waveform time derivative, i.e. the derivative skewness, is a nonlinearity/shock formation metric first identified by McInerney.<sup>13, 14</sup> The skewness of a distribution expresses asymmetry of the probability density function and accentuates outliers due to the cubed nature of the numerator. The skewness of a zero-mean variable,  $x$ , is defined as

$$\text{Sk}\{x\} = \frac{E[x^3]}{E[x^2]^{3/2}}, \quad (1)$$

where  $E[\cdot]$  represents expectation value. A skewness value of zero represents a symmetric distribution, while a positive skewness indicates the presence of a higher number of large positive values than negative. The work of Gee *et al.*<sup>15</sup> showed that the statistics of the waveform time derivative were important to perception and later quantified crackliness in terms of the derivative skewness,  $\text{Sk}\{\partial p/\partial t\}$ .<sup>16</sup> They suggested an approximate threshold of  $\text{Sk}\{\partial p/\partial t\} \geq 3$  for continuous crackle (similar to the suggestion of Reichman *et al.*<sup>17</sup> that shocks are present for  $\text{Sk}\{\partial p/\partial t\} \geq 5$ ), while a value of  $\text{Sk}\{\partial p/\partial t\} \geq 9$  indicates many significant shocks present in the waveform and is associated with high crackliness.

### B. AVERAGE STEEPENING FACTOR

The ASF<sup>18</sup> is also based on derivative values and defined as the average value of the positive derivatives over the average value of the negative derivatives:

$$\text{ASF}\{p\} = \frac{E[\dot{p}^+]}{-E[\dot{p}^-]}. \quad (2)$$

The ASF is an inverse of the previously used wave steepening factor (WSF),<sup>19</sup> so that an increase in nonlinearity corresponds to an increase in metric value. Because it involves a linear average of derivative values, ASF is less sensitive to outliers than the derivative skewness, and thus better represents average behavior. An ASF value of one corresponds to a waveform with no significant steepening, while a value above one represents some nonlinear steepening.<sup>18</sup> It has been shown that for jet noise, both full-scale<sup>20</sup> and model-scale,<sup>21</sup> an ASF value between 1.5 and 2 is indicative of the presence of shocks, with a value approaching two suggesting significant shock content.<sup>22</sup>

### C. SHOCK ENERGY FRACTION

Time-domain waveform steepening results in spectral broadening in the frequency domain, as energy is transferred from peak frequencies to higher frequencies. Although spectral broadening is often shown using the more familiar Fourier transform, a wavelet transform has been used in lab-scale jet noise analysis as a frequency-domain technique that also gives temporal resolution.<sup>21</sup> The SEF is a metric that compares high-frequency (>2 kHz for full-scale aircraft) energy associated with shocks within the waveform to the total high-frequency energy present.<sup>12</sup> A value of  $\text{SEF} = 0$  corresponds to no high-frequency energy associated with shocks, while a value of  $\text{SEF} = 1$  means that all high-frequency energy is associated with shocks.

## 4. FAR-FIELD VARIATION IN METRICS

Long-distance propagation introduces variation in metric not seen in near-field measurements; given the measurement environment, these are believed to be linked to local meteorology.

### A. UNCERTAINTY WITH DISTANCE

The waveform changes that arise due to seemingly small atmospheric changes can be dramatic. To illustrate this, three waveforms at 100% ETR from the same microphone, 22.8 m above the ground at 610 m from the MARP at an angle of 135°, are plotted in Figure 2. The three waveforms in parts (a), (b), and (c) are taken from Runs 129, 219, and 124, respectively. Although the three waveforms' OASPLs are similar: 111.2, 111.0, and 112.5 dB for the three runs in order, the waveform properties themselves look very dissimilar. The waveform in

Figure 2(a) shows several spikes that are noticeably absent from the other waveforms, and are reminiscent of sharp, positively pressure skewed, double-peak features in caustic-focused sonic booms.<sup>28</sup> The derivative skewness for the waveform in part (a) is markedly larger than the other waveforms with a value of 18.7, compared with 4.7 and 11.0 for (b) and (c). Shocks are also evident in (b) and (c), but not nearly to the extent as (a). These three waveforms help show the wide disparity in shock content that is possible at the same location due to the small atmospheric changes described in Table 1.

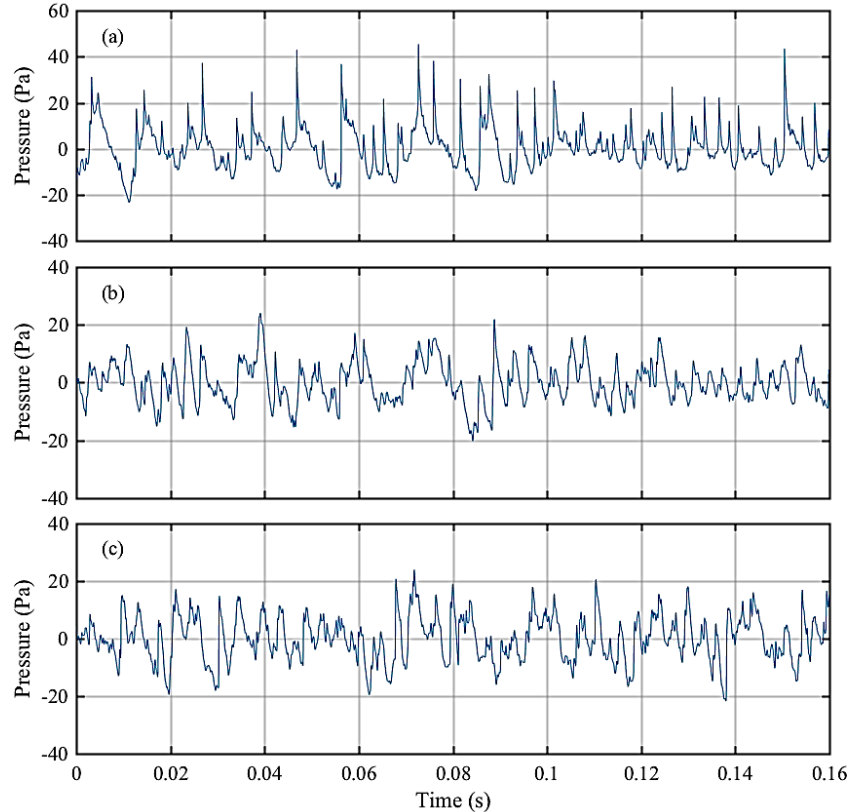


**Figure 2. Waveforms from the microphone located 22.8 m above the ground at 610 m from the MARP along the 135° radial for three runs at 100% ETR: (a) Run 129, (b) Run 219, and (c) Run 124.**

To illustrate some of the issues associated with nonlinear propagation over large distances, Figure 3 shows the mean value and standard deviation for the metrics discussed above as a function of distance along 135° for 100% ETR. Only the results from the 9.1 m microphone at 610 and 1220 m are shown here, for consistency with 76, 152, and 305 m. The OASPL, shown in Figure 3(a), is the metric that is most often used in noise modeling. The uncertainty in OASPL increases with distance, with a standard deviation of greater than 1 dB at 610 and 1220 m. Nonlinearity metric uncertainty also tends to increase with distance, but may also be compressed as nonlinearity values are reduced at greater distances.

As mentioned previously, derivative skewness values exceeding 3 suggests an important change crackliness<sup>16</sup> as shock content increases. This appears to correspond with an ASF of  $\sim 1.5$ ,<sup>20</sup> though the link between crackliness and ASF has not yet to be quantified. The derivative skewness has a large standard deviation at 305 m, but all values are above a threshold of 9, indicating continuous crackle. On the other hand, the range of values spanned by error bars in derivative skewness at 610 m and 1220 m represent a much larger range of shock content, ranging from no significant shocks to significant shocks corresponding with nearly intense crackle. The ASF values at 305 m also show a wide range of values, but all of them indicate significant shock content, while the uncertainty in ASF at 610 and 1220 m again shows that at these larger distances shock content may be significant or nearly nonexistent, depending on the run. The large uncertainty in shock content at large distances, even with weather conditions during all runs falling within the ANSI measurement standard,<sup>4</sup> points to the sensitivity of long-range propagation to small variations in atmospheric conditions.

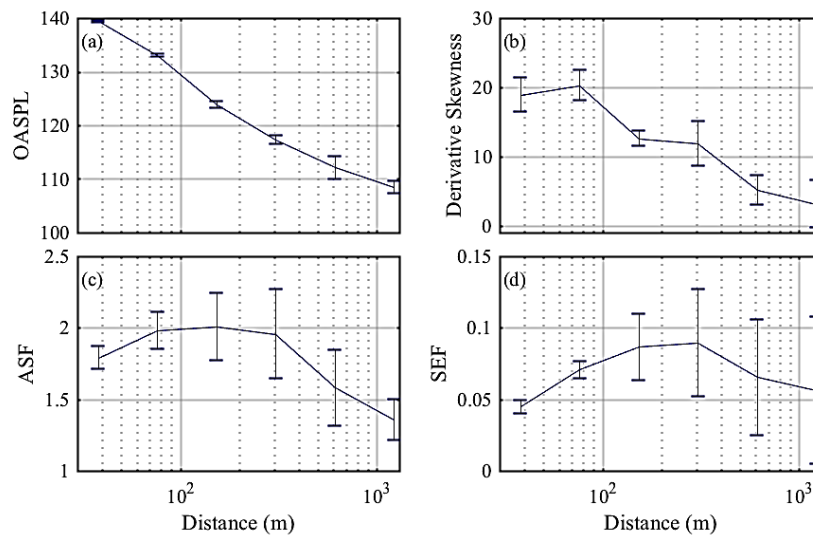


**Figure 3.** The means and standard deviations for (a) OASPL, (b) derivative skewness, (c) ASF, and (d) SEF as a function of distance along  $135^\circ$  radial for all 100% ETR runs.

Though behavior can vary in the extreme far field, during many run-ups the large derivative skewness, ASF, and SEF values indicate significant shock content at distances of 610 and 1220 m from the source. However, the variation in nonlinearity metrics suggests that there should be substantial differences in the high-frequency content at these distances as well: greater nonlinearity metric values should be associated with a marked increase in high-frequency energy. The spectra from all the microphones from 38.1 m to 1220 m along the  $135^\circ$  radial, at a height of 9.1 m, are shown in Figure 4 for all runs at 100% ETR. As expected, very little variation is seen at 38.1 m, though evidence of a ground interference null is seen near 1 kHz in some of the spectra. As distance increases, greater high-frequency variation is seen. At 610 m, one spectrum has little high-frequency content, consistently 15–20 dB below all other spectra, even though peak-frequency differences are not nearly as large. At 1220 m, differences at 200 Hz are as large as 15 dB, pointing to a secondary propagation path not due to ground reflections. (Ground reflection nulls should be located near 1 kHz according to the measurement geometry and ground impedance.) Nulls in a similar frequency range seen by Young *et al.*<sup>11</sup> for their early-morning measurements suggests a downward refracting atmosphere here for some runs, although this cannot be confirmed for this dataset. At 1220 m, some runs also exhibit significantly higher levels above 3–4 kHz, with levels in excess of 60 dB up to 10 kHz. Levels at these high frequencies and distances should be well below the noise floor due to linear absorption, indicating that even at distances as large as 1220 m, nonlinear waveform steepening is still pumping energy to high frequencies. Blackstock,<sup>23</sup> Gee and Sparrow,<sup>24</sup> and Miller *et al.*<sup>25</sup> have discussed the “old-age” nonlinear decay of jet noise and this is experimental evidence of its relevance.

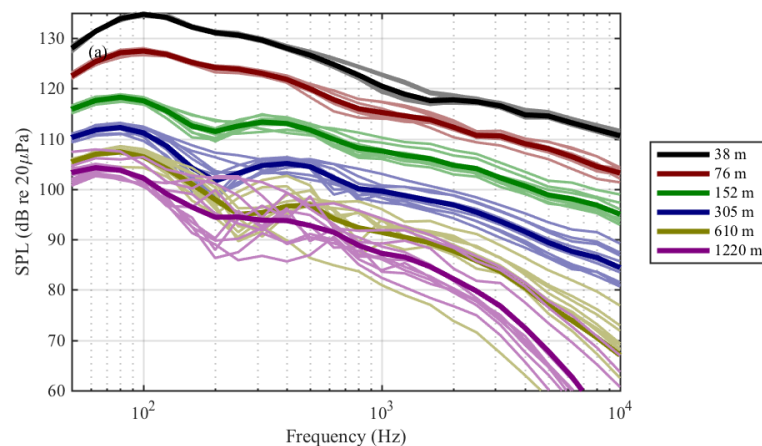


**Figure 4.** Spectra for measurement distances from 38.1 m to 1220 m along the  $135^\circ$  radial at height of 9.1 m for 100% ETR. Averaged spectrum (decibel average) at each location is shown with a darker line.

## B. HEIGHT TRENDS AT 610 m

While understanding uncertainty with distance is important, metric variation with measurement height also needs to be considered. Although most measurement locations were limited to a single height, the 610 and 1220 m measurements along the 135° radial consisted of multiple microphones at ground heights ranging from 0 to 30.1 m. The OASPLs at 610 m are plotted in Figure 5 as a function of height for all 100% ETR runs. One of the obvious trends is that, with the exception of Run 129, OASPL tends to decrease with microphone height up to 22 m, similar to results shown by McNerny *et al.*,<sup>26</sup> up to their maximum height of 12.2 m. One possible explanation for the increase in level is that near the ground, the direct transmission from the source and the ground reflection combine constructively over the peak-frequency region, but at more elevated microphones the interference can be more destructive than constructive, resulting in a lower OASPL. However, the expected ground interference nulls, even at 30 m above the ground, occur at several times the peak frequency of the noise and therefore have relatively little effect on the OASPL. This means that other long-range propagation effects due to a more complicated vertical profile in the atmosphere are the likely cause for the decrease in OASPL with microphone height.

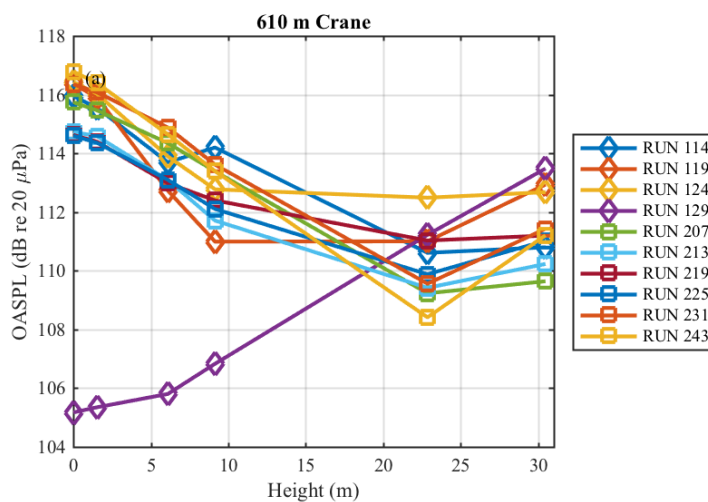


**Figure 5.** OASPL is shown as a function of height at a distance of 610 m at 135° for all runs at 100% ETR. Symbols denote which day the run was measured.

One run (Run 129) stands out within these 610 m measurements, as its OASPL increases with height. This has some precedent, as it is similar to results shown by Gee *et al.*<sup>27</sup> for a prior outdoor experiment. It is also not strictly an anomaly within the present measurement. Although not shown in Figure 5, this behavior is also seen at runs at other engine conditions immediately before and after Run 129, and the significantly lower OASPL values are also seen at the 9.1 m microphone at 120° and 150° at 610 m. While it is difficult to pinpoint exactly what meteorological conditions caused such a drastic change, it is worth noting that this run was the latest time of day of all runs at 100% ETR, and it also had the highest wind speed, as shown in Table 1. It is possible that gradients in the atmosphere at earlier times channeled the sound towards the ground, but as the ground warmed up and a temperature lapse occurred, the sound was refracted away from the ground microphones. However, a more detailed measurement of atmospheric conditions would be needed to confirm this hypothesis.

Since the OASPL is consistently lower at higher measurement locations it would be reasonable to assume nonlinearity metrics would exhibit height-dependent trends as well. Because peak frequency is consistent with height, one might assume that nonlinearity metrics would decrease for microphones with lower OASPL. Higher OASPL tends to drive shock formation, meaning that for these similar propagation paths, higher OASPL corresponds to higher values of nonlinearity metrics. Were this the case at the crane at 610 m, one would expect nonlinearity metrics to decrease with height. However, this is not the observed behavior, as shown in Figure 6. Instead, the nonlinearity metrics tend to increase with height until 22.9 m above the ground, when they decrease as OASPL increases.

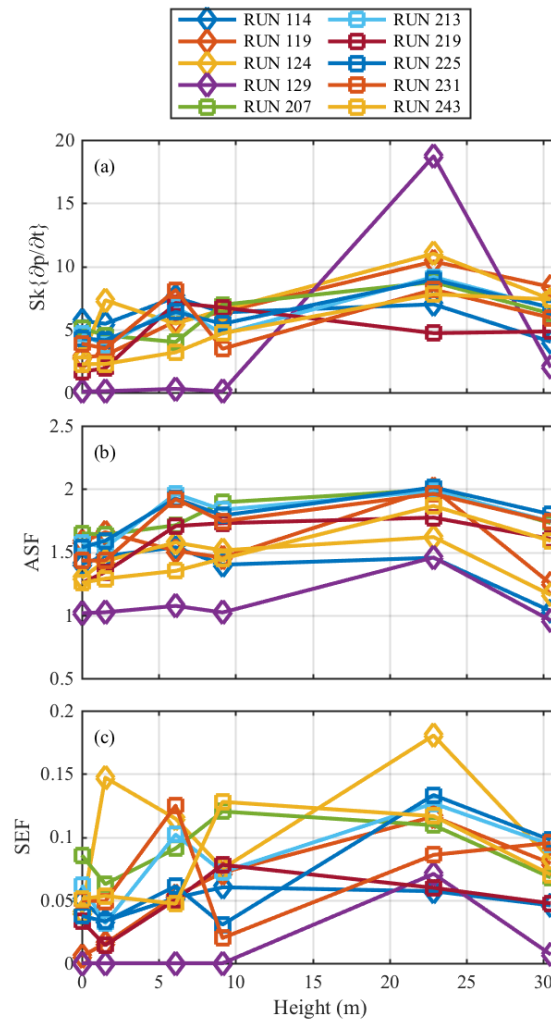


**Figure 6.** The (a) derivative skewness, (b) ASF, and (c) SEF are shown as a function of height at a distance of 610 m at 135° for all runs at 100% ETR. Symbols denote which day the run was measured.

Once again, the behavior from Run 129 is drastically different from the rest. Here, the derivative skewness up to 9.1 m is negligible, while the derivative skewness at 22.9 m (corresponding to the waveform shown in Figure 2(a)) jumps to a value of nearly 19, near the average behavior observed at 38 m and 76 m seen in Figure 3. Upon listening to these samples, the difference in sound quality is stark, with the waveform at 9.1 m having no perceived crackle, while the waveform at 22.9 m could be described as intense crackle, similar to what is heard at distances much closer to the aircraft. Just as with the OASPL behavior shown in Figure 5, this larger derivative skewness at that microphone is not limited to a single run, but is also present at other engine conditions around a similar time period. Though it is difficult to ascribe this behavior to any particular aspect of meteorological conditions, the features appear similar to the skewed peaks produced by caustic focusing, which can be caused by a downward refracting medium,<sup>8,28,29,30</sup> though the effects of continuous-noise nonlinear propagation in a downward-refracting atmosphere have not been investigated. However, it is an important finding that nonlinear propagation can be significant at distances far from the source, and that nonlinear propagation is sensitive to seemingly small ambient environment changes.

### C. HEIGHT TRENDS AT 1220 m

One way of confirming some of the trends seen at 610 m is looking for confirmation at other measurement locations, in this case using the crane at 1220 m. The trends at 610 m were for the most part unexpected, in particular the decrease in OASPL with height, with a counterintuitive increase in all three nonlinearity metrics. However, as is seen in Figure 7, the decrease in OASPL with height is accentuated further at 1220 m, with a

difference of 8-10 dB between the measurements at heights of 0 m and 30.5 m for most of the runs. However, some of the runs deviate from this behavior. Run 129 in particular shows an increase in OASPL at higher elevations, a trend that is present to a smaller degree in runs 119 and 124. Interestingly, the anomalous behavior is very different at 1220 m than at 610 m. While at 610 m, Run 129 has a 10 dB drop in OASPL at the microphones closest to the ground compared to other runs, at 1220 m the microphones near the ground are unchanged, and elevated microphones see a large increase in OASPL. This implies that the atmospheric conditions create a “shadow zone” at lower microphones at 610 m during Run 129, but the sound is again refracted toward the ground by 1220 m. Regardless, the findings from Figure 7 confirm the behavior seen in Figure 5, that for the course of most of the experiment the OASPL decreases with microphone heights, far more so than would be expected for straight-ray propagation.

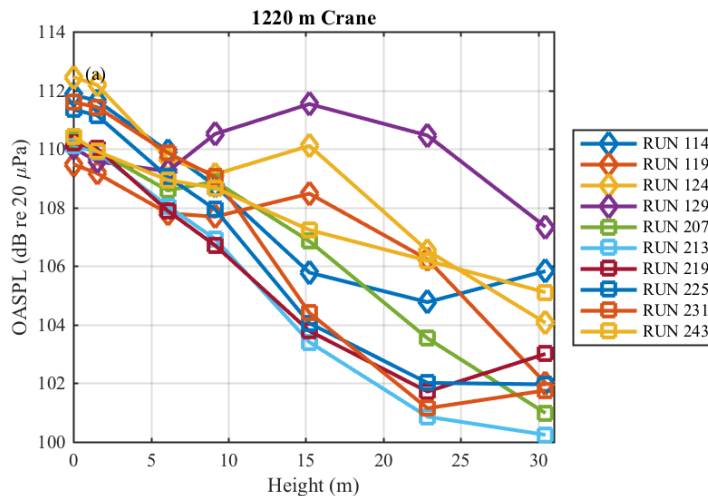


**Figure 7.** OASPL is shown as a function of height at a distance of 1220 m at  $135^\circ$  for all runs at 100% ETR. Symbols denote which day the run was measured.

The other unexpected trend seen at 610 m was the increase in nonlinearity metrics corresponding to the decrease in OASPL with height. Once again, this trend is confirmed by comparing the behavior at the 1220 m crane with that of the 610 m crane. The trend seen in Figure 8 is similar to the behavior in Figure 6, that nonlinearity metrics tends to increase with height, though this is not as clear as in Figure 6, and nonlinearity metrics peak at lower heights for many of the runs. It is also important to note that the values of the nonlinearity metrics still indicate the presence of significant shocks and crackle. While derivative skewness values vary wildly, in particular at higher microphones, values of 3-5 are seen in roughly half the runs at 22.9 and 30.5 m, indicating continuous crackle and significant shock content.<sup>31</sup> Also important to note is the high derivative skewness values associated with runs 129 and 243. These show the sensitivity of nonlinear propagation to weather effects over long-range propagation and point to the need for better understanding of how changes in the atmosphere within the measurement standard can lead to significantly stronger shocks at some locations.

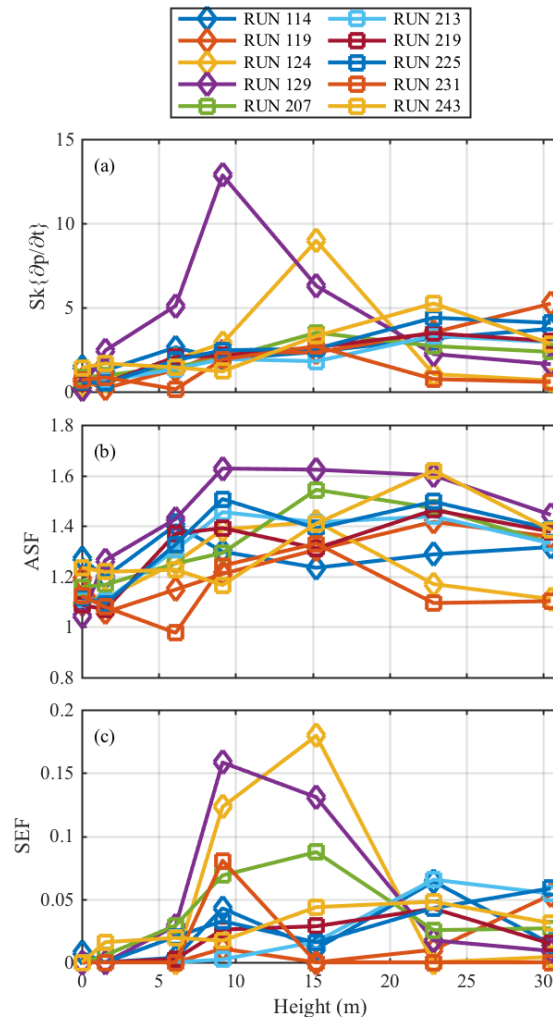


Figure 8. The (a) derivative skewness, (b) ASF, and (c) SEF are shown as a function of height at a distance of 1220 m at  $135^\circ$  for all runs at 100% ETR. Symbols denote which day the run was measured.

## 5. VARIATION ATTRIBUTABLE TO ATMOSPHERIC CONDITIONS

Since near-field measurements of OASPL in Figure 3 have a standard deviation of less than 1 dB, the larger variation in OASPL at distances far from the source is likely due to small changes in atmospheric conditions. Though a lack of atmospheric data limits analyses, a connection between weather measurements and trends in OASPL would help explain some of the result seen in Section 4. While the weather data collected during the experiments were limited, anomalous behavior at the 610 and 1220 m microphones can be connected to quantities such as average wind, the time of day, and a possible temperature inversion.

One of the issues in extracting trends as a function of height from the available data is the small number of runs at each ETR. While variation is seen in the OASPL values in Figure 5, nine or ten runs is likely not enough to show the entire range of possible behavior. To show a larger dataset, OASPL data from all engine conditions are plotted in Figure 9. To compare weather effects, rather than effects due to engine condition, these OASPL values have been normalized to the mean OASPL at a height of 0 m at each engine condition. For instance, the OASPL curves from Figure 5 have had a value of 116 dB subtracted. Unfortunately, normalizing nonlinearity metrics is not as insightful given the wide range of values at each engine condition, and so the analyses in this section are confined to OASPL.

The OASPL at all microphone heights at distances of 610 m and 1220 m and over a range of engine conditions from 75% (Intermediate) to 150% ETR (Maximum afterburner) are shown in Figure 9, with the color of the line corresponding to the average wind speed over the course of the run. Many of the trends seen in Figure 5 and Figure 7 are immediately apparent, showing they are not limited to 100% ETR. For the majority of the

cases, the OASPL decreases with height, with a difference of  $\sim 5$  dB between 0 and 30.5 m for the crane at 610 m and a difference of 7-10 dB at the 1220 m crane. Also apparent are a few curves that display anomalous behavior, similar to Run 129 shown in Figure 5. These curves show that this behavior was not limited to a single contaminated measurement. It is interesting to note that a higher wind speed occurs during all of these events which deviate from the trend of decreasing OASPL with height observed during the rest of the measurement. However, not all high-wind events result in atypical behavior; while a high wind speed is likely related to the occurrence of the anomalous behavior, it is not enough to predict the behavior alone.

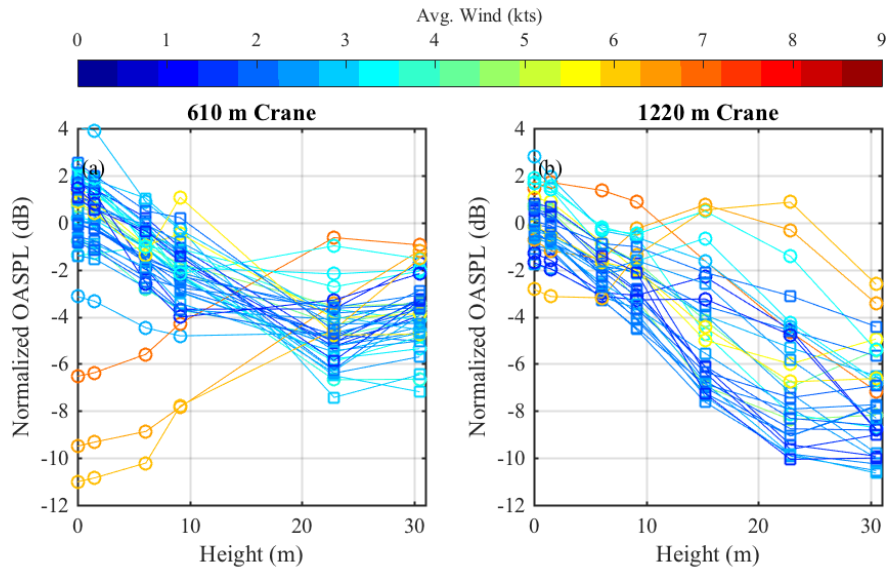


**Figure 9.** The OASPL (Normalized to average level at 0 m height at each engine condition) as a function of height for all engine conditions from 75% to 150% ETR at 135°. Colors correspond to average wind throughout the run.

Wind is not the only factor that can have a large influence on long-range propagation. Another variable to consider is atmospheric stratification. While small variations in temperature are not likely to alter propagation significantly themselves, changes in temperature gradients may have a larger impact. Unfortunately, the weather data from these measurements makes it difficult to say conclusively when there was a temperature inversion or lapse, though previous measurements suggest a transition to a temperature lapse occurring with the first 30 minutes after sunrise.<sup>32</sup> However, the time of day is likely related to changes in these atmospheric conditions, and in particular, the transition from a possible temperature inversion to a temperature lapse as the sun rises.

To help demonstrate the effect of time of day, Figure 10 below shows the same OASPL curves as a function of height seen in Figure 9, but the colors now correspond to local time. Sunrise occurred at 6:28 AM on both measurement days, and it is likely that if a temperature inversion were present, it would turn into a temperature lapse as the ground is heated shortly after sunrise, possibly within the first 30 minutes. Similar to the trends seen with wind in Figure 9, all of the anomalous curves occur at times later in the day, with what appears to be an even stronger relationship than for wind speed. However, once again the time of day is not a perfect predictor of OASPL behavior. Observed long-range propagation effects are a combination of temperature and wind profiles, and more detailed weather data are needed to uncover a relationship between atmospheric conditions and propagation effects.

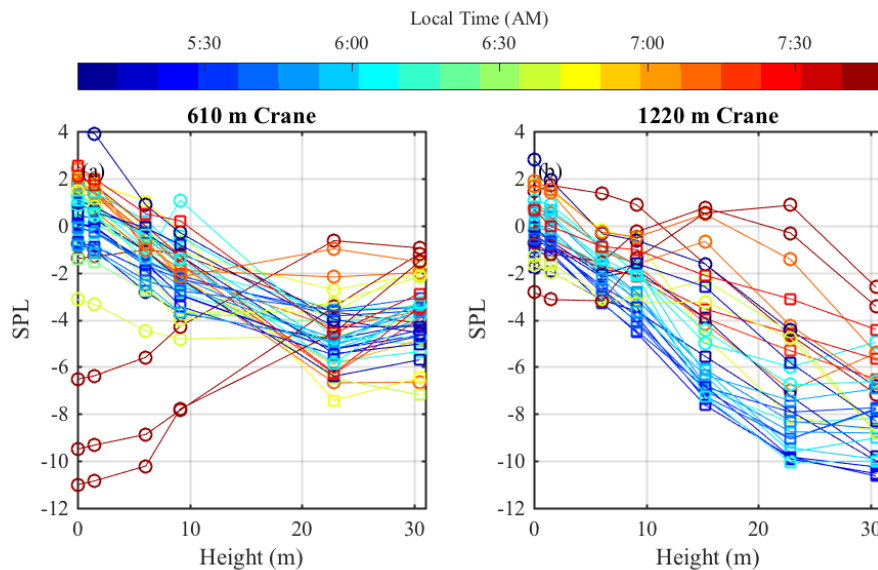


**Figure 10.** The OASPL (Normalized to average level at 0 m height at each engine condition) as a function of height for all engine conditions from 75% to 150% ETR at 135°. Colors correspond to measurement time.

## 6. CONCLUSIONS AND FUTURE WORK

This paper has illustrated the importance that nonlinear propagation can have at large distances from high-power, tactical jet aircraft, but also the difficulties in accounting for the effect of atmospheric conditions on long-range acoustic propagation. Over two days, measurements at 100% ETR, all with weather conditions within ranges allowed by the measurement standard, have consistent OASPL, spectra, and nonlinearity metrics close to the aircraft but exhibit wide-ranging behavior at distances of 305 m and greater. One fairly consistent trend seen at microphones located at 610 and 1220 m from the source is a decrease in OASPL with measurement height and an unexpected rise in nonlinearity metrics. However, some variations are seen from these trends. Atmospheric conditions occasionally produce a much lower OASPL than expected or greater nonlinearity metric values. The anomalous behavior is not limited to a single event, but all events exhibiting the behavior occur later in the morning on the first day of measurement and are associated with higher wind speeds. This behavior suggests a transition from a downward-refracting atmosphere to an upward-refracting atmosphere, likely due to changes in temperature and wind shortly after sunrise. While previous measurements support this idea, more precise meteorological data are needed to associate changes in the far-field metrics with smaller atmospheric changes.

## ACKNOWLEDGMENTS

The authors gratefully acknowledge funding for the measurements provided through the F-35 Program Office and Air Force Research Laboratories. (Distribution A—Approved for Public Release; Distribution is Unlimited; Cleared 11/02/2018; JSF18-1022.) B. O. Reichman was funded by an appointment to the Student Research Participation Program at the U.S. Air Force Research Laboratory, 711th Human Performance Wing, Human Effectiveness Directorate, Warfighter Interface Division, Battlespace Acoustics Branch, administered by the Oak Ridge Institute for Science and Education through an interagency agreement between the U.S. Department of Energy and U.S. Air Force Research Laboratory.

## REFERENCES

- <sup>1</sup> M. M. James, A. R. Salton, J. M. Downing, K. L. Gee, T. B. Neilsen, B. O. Reichman, R. L. McKinley, A. T. Wall, and H. L. Gallagher, "Acoustic Emissions from F-35 Aircraft during Ground Run-Up," AIAA Paper 2015-2375 (2015).
- <sup>2</sup> U. Ingard, "A Review of the Influence of Meteorological Conditions on Sound Propagation," J. Acoust. Soc. Am. 25, 405 (1953).

- 
- <sup>3</sup> J. E. Piercy, T. F. W. Embleton, and L. C. Sutherland, "Review of noise propagation in the atmosphere," *J. Acoust. Soc. Am.* 61, 1403 (1977).
- <sup>4</sup> ANSI/ASA, "Methods for the Measurement of Noise Emissions from High Performance Military Jet Aircraft," S12.75 (2012).
- <sup>5</sup> D. T. Blackstock, "Fundamentals of physical acoustics," John Wiley & Sons, Inc, 2000.
- <sup>6</sup> K. Attenborough, S. Taherzadeh, H. E. Bass, X. Di, R. Raspet, G. R. Becker, A. Güdesen, A. Chrestman, G.A. Daigle, A. L'Espérance, Y. Gabillet, K. E. Gilbert, Y. L. Li, M. J. White, P. Naz, J. M. Noble, and H. A. J. M. van Hoof, "Benchmark cases for outdoor sound propagation models," *J. Acoust. Soc. Am.* 97, 173 (1995); doi: 10.1121/1.412302
- <sup>7</sup> D. K. Wilson, "The sound-speed gradient and refraction in the near-ground atmosphere," *J. Acoust. Soc. Am.* 113, 750 (2003).
- <sup>8</sup> E. K. Salomons, "Computational atmospheric acoustics," Kluwer Academic Publishers, 2001.
- <sup>9</sup> P. J. Dickinson, "Temperature inversion effects on aircraft noise propagation," *J. Sound and Vib.* 47 (3), pp. 438-443 (1976).
- <sup>10</sup> T. F. W. Embleton, "Tutorial on sound propagation outdoors," *J. Acoust. Soc. Am.* 100, 31 (1996).
- <sup>11</sup> S. M. Young, K. L. Gee, T. B. Neilsen, and K. M. Leete, "Outdoor measurements of spherical acoustic shock decay," *J. Acoust. Soc. Am.* 138, EL305 (2015).
- <sup>12</sup> B. O. Reichman, K. L. Gee, T. B. Neilsen, and S. H. Swift, "Acoustic shock formation in noise propagation during ground run-up operations of military aircraft," AIAA Paper 2017-4043 (2017).
- <sup>13</sup> S. A. McNerny, "Launch vehicle acoustics. II-Statistics of the time domain data," *J. of Aircraft* 33, 518-523 (1996).
- <sup>14</sup> S. A. McNerny, M. Downing, C. Hobbs, M. James, and M. Hannon, "Metrics that characterize nonlinearity in jet noise," AIP Conference Proceedings 838, 560-563 (2006).
- <sup>15</sup> K. L. Gee, V. W. Sparrow, A. A. Atchley, and T. B. Gabrielson, "On the perception of crackle in high-amplitude jet noise," *AIAA J.* 45, 593-598 (2007).
- <sup>16</sup> K. L. Gee, P. B. Russavage, T. B. Neilsen, S. H. Swift, and A. B. Vaughn, "Subjective rating of the jet noise crackle percept," *J. Acoust. Soc. Am.* 144(1), EL40-EL45 (2018)
- <sup>17</sup> B. O. Reichman, M. B. Muhlestein, K. L. Gee, T. B. Neilsen, and D. C. Thomas, "Evolution of the time-derivative skewness of nonlinearly propagating waves," *J. Acoust. Soc. Am.* 139, 1390-1403 (2016).
- <sup>18</sup> M. B. Muhlestein, K. L. Gee, T. B. Neilsen, and D. C. Thomas, "Evolution of the average steepening factor for nonlinearly propagating waves," *J. Acoust. Soc. Am.* 137, 640-650 (2015).
- <sup>19</sup> J. Gallagher, "The effect of non-linear propagation in jet noise," AIAA 20th Aerospace Sciences Meeting (1982).
- <sup>20</sup> K. L. Gee, T. B. Neilsen, A. T. Wall, J. M. Downing, M. M. James, R. L. McKinley, "Propagation of crackle-containing jet noise from high-performance engines," *Noise Control. Eng. J.* 64, 1-12 (2016).
- <sup>21</sup> W. J. Baars and C. E. Tinney, "Shock-structures in the acoustic field of a Mach 3 jet with crackle," *J. Sound and Vib.* 12, 2539-2553 (2014).
- <sup>22</sup> K. L. Gee, T. B. Neilsen, J. M. Downing, M. M. James, R. L. McKinley, R. C. McKinley, and A. T. Wall, "Near-field shock formation in noise propagation from a high-power jet aircraft," *J. Acoust. Soc. Am.* 133, EL88-EL93 (2013).
- <sup>23</sup> D. T. Blackstock, "Once nonlinear, always nonlinear," AIP Conf. Proc. 838, 601-606 (2006).
- <sup>24</sup> K. L. Gee and V. W. Sparrow, "Asymptotic behavior in the numerical propagation of finite-amplitude jet noise," AIP Conf. Proc. 838, 564-567 (2006).
- <sup>25</sup> K. G. Miller, K. L. Gee, and B. O. Reichman, "Asymptotic behavior of a frequency-domain nonlinearity indicator for solutions to the generalized Burgers equation," *J. Acoust. Soc. Am.* 140, EL522-EL527 (2016).
- <sup>26</sup> S. McNerny, K. L. Gee, M. J. Downing, and M. M. James, "Acoustical Nonlinearities in Aircraft Flyover Data," AIAA Paper No. 2007-3654.
- <sup>27</sup> K. L. Gee, V. W. Sparrow, M. M. James, J. M. Downing, and C. M. Hobbs, "Measurement and prediction of nonlinearity in outdoor propagation of periodic signals," *J. Acoust. Soc. Am.* 120 (5), 2491-2499 (2006).
- <sup>28</sup> K. J. Plotkin, "State of the art sonic boom modeling," *J. Acoust. Soc. Am.* 111, 530 (2002).
- <sup>29</sup> R. Marchiano, F. Coulouvrat, and R. Grenon, "Numerical simulation of shock wave focusing at fold caustics, with application to sonic boom," *J. Acoust. Soc. Am.* 114, 1758 (2003).
- <sup>30</sup> B. Lipkens and D. T. Blackstock, "Model experiment to study sonic boom propagation through turbulence. Part I: General results," *J. Acoust. Soc. Am.* 103, 148 (1998).
- <sup>31</sup> K. L. Gee, T. B. Neilsen, A. T. Wall, J. M. Downing, M. M. James, R. L. McKinley, "Propagation of crackle-containing jet noise from high-performance engines," *Noise Control. Eng. J.* 64, 1-12 (2016).
- <sup>32</sup> K. L. Gee, "Prediction of nonlinear jet noise propagation," PhD Dissertation, Pennsylvania State University (2005).